Off-resonance regimes in nonlinear quantum Rabi models

V. Penna[1,2] and F. A. Raffa[1]

[1]*Dipartimento di Scienza Applicata e Tecnologia Politecnico di Torino, Corso Duca degli Abruzzi 24, I-10129 Torino, Italy*

[2]*U.d.r. CNISM, Politecnico di Torino, Corso Duca degli Abruzzi 24, I-10129 Torino, Italy*

(Received 11 November 2015; published 8 April 2016)

We study the nonlinear quantum Rabi model—both in the two-photon and the intensity-dependent coupling scheme—by utilizing the perturbation method in the off- and near-resonance regimes characterized by the field and the atomic transition frequencies. We consider the weak-coupling condition, the perturbation parameter being the ratio between the coupling constant and the atomic frequency. For both models we determine the first- and second-order corrections to energy eigenvalues and eigenstates, disclosing the doublet structure characterizing the energy spectrum. Then we apply our findings to both the coupling schemes in order to calculate the time evolution of a general initial state and the atomic population inversion for an initial state composed by a mixture of excited and unexcited atoms.

DOI: 10.1103/PhysRevA.93.043814

I. INTRODUCTION

The quantum Rabi model provides a simple but successful paradigm of the interaction between matter and electromagnetic fields where a matter qubit, a two-level atom, interacts with a single field mode. After the seminal papers [1], where radiation was considered within the semiclassical limit, extensive use of the quantum Rabi model and its manifold applications in quantum optics [2,3], quantum information [4], and atom physics [5] are well documented, and include, on a more theoretic ground, a recent considerable interest for its integrability properties [6–11].

Two nonlinear generalizations of the quantum Rabi model are well known in which the field-atom interaction of the model Hamiltonian, involving two different realizations of algebra su(1,1), can be written in a unified form resorting to the ladder operators $K_\pm$ of the algebra.

Selecting the Schwinger realization [12] for $K_\pm$ leads to the two-photon quantum Rabi model (TPM), where the absorption and emission mechanism, featuring two photons rather than one, has been thoroughly studied and used in physical applications, as reported, e.g., in [13,14]. From a theoretical point of view, the search for analytical solutions of the two-photon model (see, e.g., [15] and references therein) has been significantly revamped since Braak presented his solution scheme [6] for the one-photon quantum Rabi model, which is based on the Bargmann representation of boson operators a and $a^\dagger$.

This intense investigation includes the solution of the TPM through the extension of Braak's approach [7,8], the TPM characterized by the presence of two qubits and their mutual interaction [9], and the extension of the TPM to a multiqubit chain via trapped-ion technology, which reveals the effect of the coupling-induced spectral collapse [10]. A diagonalization scheme based on a symmetric form of the rotating-wave approximation is reported in [11].

On the other hand, using the Holstein-Primakoff realization [16,17] for operators $K_\pm$ results in the intensity-dependent Rabi model (IDM), a kind of nonlinear light-matter coupling whose definition, within the frame of the Jaynes-Cummings model (JCM) [18], can be traced back to works [19,20]. Numerical investigations [21,22] are usually carried out for analyzing this coupling, whose experimental realization has been achieved recently by studying the light transport in engineered waveguide superlattices [23–25]. The IDM, including m-photon processes with $m \geqslant 2$, has been considered in [26].

Unlike the cited works, which rely mainly on numerical approaches or appropriate extensions of Braak's semianalytical scheme, in this work we analyze the nonlinear TPM and IDM by resorting to the standard perturbative approach [27]. The advantage is that implementing a fully analytic treatment of the problem provides a description of the physical properties that explicitly depends on the model parameters. We note in advance that the perturbative approach implicitly excludes the resonance condition between the atomic and the field-mode frequencies. Then, in this paper, our attention is focused on both the off- and near-resonance regimes of the system without applying the rotating-wave approximation.

We determine the second-order expressions of the energy eigenvalues and of the corresponding eigenstates, which provides a deeper insight into the interplay among the model parameters and suggests prospective physical phenomenology. Based on these results we show how, for both the TPM and the IDM, the spectrum features different energy-doublet structures depending on the model-parameter regime one considers. Then, we calculate the explicit expressions for the time evolution of a generic quantum state and apply this finding to illustrate the time behavior of the atomic population inversion (API) in the case when the initial state of the system corresponds to a superposition of excited and unexcited atomic states.

While our analysis is mainly devoted to the dynamical aspects of the TPM in view of its relevance in fully quantum systems, we note that the very generality of the perturbative scheme allows for a straightforward extension of this scheme to the IDM, which we perform in the final part of the paper.

For this reason we have structured our work as follows: First, we detail the su(1,1) framework of both models in Sec. II, while reporting in Sec. III the relevant second-order perturbative results (energy eigenvalues and eigenstates) in the weak-coupling regime. In the latter section we resort to a perturbation scheme, which proved useful already for trapped ions [28]. For the TPM we derive the evolution of the model quantum state (Sec. IV) and evaluate API

in Sec. V. In our time-dependent analysis the initial state of the system is considered to be a superposition of two number-spin product states. In Sec. VI we report the results for the IDM, while Sec. VII is devoted to concluding remarks. Additional mathematical details are supplemented in the Appendices.

II. PERTURBATIVE APPROACH TO NONLINEAR RABI MODEL

In units $\hbar = 1$, the TPM and the IDM are both embodied in the Hamiltonian

$$H = \omega\hat{n} + \omega_0 S_3 + g(K_- + K_+)(S_+ + S_-), \tag{1}$$

where g is the coupling constant, and ω and ω_0 denote the energy of the bosonic-field mode and the atomic transition energy, respectively. In Eq. (1) pseudospin operators S_3 and $S_\pm$ act on the two-dimensional atomic space, K_- and K_+ are ladder operators acting on the field Fock space, and $\hat{n} = a^\dagger a$ with $[a,a^\dagger] = 1$. Operators S_3, $S_\pm$ and K_3, $K_\pm$ represent the standard generators of algebras su(2) and su(1,1), respectively, obeying well-known commutation relations [29]. Hamiltonian (1) comprises both nonlinear quantum Rabi models and their explicit expressions, depending on the realization of operators $K_\pm$ one works with. Resorting to the single-mode Schwinger realization [30] of the su(1,1) generators,

$$K_- = \tfrac{1}{2}a^2, \quad K_+ = K_-^\dagger, \quad K_3 = \tfrac{1}{2}\big(\hat{n} + \tfrac{1}{2}\big), \tag{2}$$

model (1) yields the TPM, while in the frame of the single-mode Holstein-Primakoff realization [16,17]

$$K_- = \sqrt{\hat{n} + 2\kappa}\, a, \quad K_+ = K_-^\dagger, \quad K_3 = \hat{n} + \kappa, \tag{3}$$

with κ the group-representation index, the IDM is retrieved from Hamiltonian (1).

The general form of Eq. (1), suitable to a perturbative approach, is

$$H = H_{\rm unp} + \varepsilon W, \tag{4}$$

where $H_{\rm unp}$ is the unperturbed Hamiltonian, ε the perturbation parameter, and the perturbative term W assumes different expressions depending on the coupling scheme. We identify the perturbation parameter of model (1) with the dimensionless ratio $\varepsilon = g/\omega_0$, so that in Eq. (4)

$$H_{\rm unp} = \omega\hat{n} + \omega_0 S_3, \tag{5}$$

and

$$W = \frac{\omega_0}{2}(a^2 + a^{\dagger 2})(S_+ + S_-), \tag{6}$$

$$W = \omega_0(\sqrt{\hat{n} + 2\kappa}\, a + a^\dagger\sqrt{\hat{n} + 2\kappa})(S_+ + S_-), \tag{7}$$

in the coupling schemes corresponding to the operator realizations (2) and (3), respectively. Following the stationary perturbation theory [27] for the eigenvalue problem $H|E(n,s)\rangle = E(n,s)|E(n,s)\rangle$, one expands both eigenvalues and eigenstates $E(n,s)$ and $|E(n,s)\rangle$ in powers of ε, where $s = \pm 1$ is the quantum number associated to the atomic states, i.e., $S_3|s\rangle = (s/2)|s\rangle$, while index $n \in \mathbb{N}_0$ labels the field-mode states such that $\hat{n}|n\rangle = n|n\rangle$. For completeness, we report here the standard formulas of perturbation theory which we have utilized in our first- and second-order analysis,

$$E_1(n,s) = \langle E_0(n,s)|W|E_0(n,s)\rangle, \tag{8}$$

$$|E_1(n,s)\rangle = \sum_{m\neq n}\sum_r \frac{\langle m,r|W|n,s\rangle}{E_0(n,s) - E_0(m,r)}\,|m,r\rangle, \tag{9}$$

$$E_2(n,s) = \sum_{m\neq n}\sum_r \frac{|\langle m,r|W|n,s\rangle|^2}{E_0(n,s) - E_0(m,r)}, \tag{10}$$

$$|E_2(n,s)\rangle = \sum_{m\neq n}\sum_r \frac{|\langle m,r|W|E_1(n,s)\rangle|^2}{E_0(n,s) - E_0(m,r)}|m,r\rangle. \tag{11}$$

In the previous formulas the spin index r takes the value ± 1, while the eigenvalue $E_0(n,s)$ and the relevant eigenstate $|E_0(n,s)\rangle$, entering the unperturbed problem $H_{\rm unp}|E_0(n,s)\rangle = E_0(n,s)|E_0(n,s)\rangle$, are given by

$$E_0(n,s) = \omega n + \tfrac{1}{2}\omega_0 s, \quad |E_0(n,s)\rangle = |n,s\rangle. \tag{12}$$

Note that the unperturbed eigenstates simply represent the direct product of a photon state and an atomic state, namely, $|n,s\rangle = |n\rangle|s\rangle$, $|m,r\rangle = |m\rangle|r\rangle$.

III. PERTURBATIVE RESULTS FOR THE TWO-PHOTON MODEL

The first-order contribution to the eigenvalues and eigenvectors of the TPM are easily found to be

$$E_1(n,s) = 0$$

and

$$|E_1(n,s)\rangle = \frac{\omega_0}{2}\left[\frac{b_n|n-2\rangle}{2\omega + \omega_0 s} - \frac{b_{n+2}|n+2\rangle}{2\omega - \omega_0 s}\right]|-s\rangle, \tag{13}$$

with $b_n = \sqrt{n(n-1)}$, respectively. Determining second-order contributions requires a longer but straightforward calculation, leading to the expressions

$$E_2(n,s) = \frac{\omega_0}{2}\left[q(s)\binom{n}{2} - q(-s)\binom{n+2}{2}\right] \tag{14}$$

where

$$q(\pm s) = \frac{\omega_0}{2\omega \pm \omega_0 s}, \tag{15}$$

and

$$\begin{aligned}|E_2(n,s)\rangle &= \frac{1}{8}\frac{\omega_0}{\omega}[q(s)K_-^2 + q(-s)K_+^2]|n\rangle|s\rangle,\\ &= \frac{1}{16}\frac{\omega_0}{\omega}[q(s)c_n|n-4\rangle + q(-s)c_{n+4}|n+4\rangle]|s\rangle,\end{aligned} \tag{16}$$

with $c_n = \sqrt{n!/(n-4)!}$.

A. Spectrum properties in the off-resonance regime

The energy eigenvalues including correction (14) have the form

$$E(n,s) = E_0(n,s) + \frac{\varepsilon^2\omega_0^2}{4}\left[\frac{n(n-1)(2\omega-\omega_0 s)}{4\omega^2-\omega_0^2} - \frac{(n+1)(n+2)(2\omega+\omega_0 s)}{4\omega^2-\omega_0^2}\right], \tag{17}$$

which implicitly defines two off-resonance regimes, $2\omega < \omega_0$ and $2\omega > \omega_0$. Both can exhibit doublet structures of energy levels, even if originated differently. Indeed, in the first case, by assuming $\omega_0 = p\omega$ with integer $p > 2$, one naturally finds the degeneracy condition

$$E_0(n,+1) = E_0(m,-1)$$

of the unperturbed levels, if $p = m - n$. Eigenvalues $E_0(n,+1)$ and $E_0(n+p,-1)$ are thus grouped into a $s = +1$ band and $s = -1$ band, respectively, whose lowest levels $n = 0$ and $m = 0$ are shifted of ω_0. The resulting spectrum, formed by levels $E(n,s)$ including the second-order corrections, is characterized by interband level doublets with $E(n,+1)$ and $E(n+p,-1)$, whose gap

$$E(m,-1) - E(n,+1) = \frac{\varepsilon^2\omega_0^2}{2(4\omega^2-\omega_0^2)}\gamma(m,n),$$

with $m = n + p$ and $\gamma(m,n) = \omega_0(m^2+n^2+m+n+2) - 4\omega p$, is controlled by the perturbation parameter ε.

A different type of doublet structure appears, in the second case, when the condition $2\omega > \omega_0$ becomes a strong inequality $2\omega \gg \omega_0$. The latter, in fact, implies a quasidegeneracy condition in that $E_0(n,+1) - E_0(n,-1) = \omega_0 \ll \omega$. The energy gap of perturbed levels reads

$$E(n,+1) - E(n,-1) = \omega_0\left[1 - \varepsilon^2\frac{n^2+n+1}{4(\omega/\omega_0)^2-1}\right]$$

when second-order contributions are considered. In this limiting regime the occurrence of level doublets represents a property of the unperturbed energies. Second-order terms simply represent perturbative corrections of the level separation ω_0.

IV. TIME PROPAGATION OF STATES FOR THE TWO-PHOTON MODEL

The scheme we use for determining the time propagation of a generic unperturbed eigenstate $|E_0(m,r)\rangle = |m\rangle|r\rangle$ and including second-order corrections is described in Appendix A. By exploiting the expressions for $E_0(n,s)$, $E_2(n,s)$, $|E_1(n,s)\rangle$, and $|E_2(n,s)\rangle$, Eq. (A1) can be reduced to the form

$$\begin{aligned}|\psi_t(m,r)\rangle = e^{-iHt}|m\rangle|r\rangle \simeq e^{-i[E_0(m,r)+\varepsilon^2E_2(m,r)]t}&\left[1+\frac{\varepsilon^2}{2}(V_t(r,m,\varepsilon)+V_t'(r,m,\varepsilon))\right]|m\rangle|r\rangle\\ &+\frac{\varepsilon^2}{2}(e^{-4i\omega t}U_t(r,m,\varepsilon)|m+4\rangle|r\rangle + e^{4i\omega t}U_t'(r,m,\varepsilon)|m-4\rangle|r\rangle)\\ &+\frac{\varepsilon}{\sqrt{2}}q(r)\binom{m}{2}^{\frac{1}{2}}[1-e^{-i\varepsilon^2\Delta E_2(m-2,-r)t}e^{+i(2\omega+\omega_0 r)t}]|m-2\rangle|-r\rangle\\ &-\frac{\varepsilon}{\sqrt{2}}q(-r)\binom{m+2}{2}^{\frac{1}{2}}[1-e^{-i\varepsilon^2\Delta E_2(m+2,-r)t}e^{-i(2\omega-\omega_0 r)t}]|m+2\rangle|-r\rangle,\end{aligned} \tag{18}$$

where $\Delta E_2(m\pm q,\pm r) = E_2(m\pm q,\pm r) - E_2(m,r)$, with $q = 2,4$ (note that the double signs of r and of q are independent from each other), and the time-dependent quantities

$$\begin{aligned}U_t(r,m,\varepsilon) &= \sqrt{6}\binom{m+4}{4}^{\frac{1}{2}}\left[\frac{\omega_0}{4\omega}(e^{4i\omega t}q(-r)+e^{-i\varepsilon^2\Delta E_2(m+4,+r)t}q(r)) - e^{-i\varepsilon^2\Delta E_2(m+2,-r)t}\,\frac{\omega_0^2e^{i(2\omega+\omega_0 r)t}}{4\omega^2-\omega_0^2}\right],\\ U_t'(r,m,\varepsilon) &= \sqrt{6}\binom{m}{4}^{\frac{1}{2}}\left[\frac{\omega_0}{4\omega}(e^{-4i\omega t}q(r)+e^{-i\varepsilon^2\Delta E_2(m-4,+r)t}q(-r)) - e^{-i\varepsilon^2\Delta E_2(m-2,-r)t}\,\frac{\omega_0^2e^{-i(2\omega-\omega_0 r)t}}{4\omega^2-\omega_0^2}\right],\\ V_t(r,m,\varepsilon) &= q^2(r)\binom{m}{2}(e^{-i\varepsilon^2\Delta E_2(m-2,-r)t}e^{i(2\omega+\omega_0 r)t}-1),\\ V_t'(r,m,\varepsilon) &= q^2(-r)\binom{m+2}{2}(e^{-i\varepsilon^2\Delta E_2(m+2,-r)t}e^{-i(2\omega-\omega_0 r)t}-1),\end{aligned}$$

have been introduced. It is worth noting that both formula (18) and the subsequent definitions feature two time scales corresponding to

$$T_\pm = \frac{2\pi}{|2\omega\pm\omega_0|},\quad T_\varepsilon \sim \frac{2\pi}{\varepsilon^2\Delta E_2(m\pm q,\pm r)}. \tag{19}$$

The fact that $T_\pm \ll T_\varepsilon$ implies that the exponential terms depending on $\Delta E_2(m \pm q, \pm r)$ essentially exhibit no time dependence for times $t \sim T_\pm$.

Within this time scale, formula (18) shows that the main perturbative contribution to the time evolution of a state with definite spin r (atomic level) is a first-order term corresponding to a state with opposite spin $-r$. If one assumes, for example, $r = -1$ and considers ω of the same order of $\omega_0/2$, the main perturbative contribution in $|\psi(t)\rangle$ corresponds to the state $|m-2\rangle|+1\rangle$ exhibiting a slowly oscillating coefficient containing the term $q(-1)$. The latter can be significantly larger than $q(+1)$ included in the rapidly oscillating coefficient of $|m+2\rangle|+1\rangle$. The atomic excitation through the destruction of two photons thus represents the favored process with the initial state $|m\rangle|-1\rangle$. On the other hand, consistent with this reasoning, state $|m+2\rangle|-1\rangle$ (emission of two photons from an excited atom) is the principal perturbative contribution when assuming $r = +1$, namely, the initial state $|m\rangle|+1\rangle$.

In passing, we note that, owing to formula (18), one can calculate the time propagation

$$|\Psi_t\rangle = e^{-iHt}\sum_s\sum_n f_{n,s}|n\rangle|s\rangle = \sum_s\sum_n f_{n,s}(t)|n\rangle|s\rangle,$$

of the more general initial state $\sum_s\sum_n f_{n,s}|n\rangle|s\rangle$, representing a superposition of photonic and spin states.

V. ATOMIC POPULATION INVERSION FOR THE TWO-PHOTON MODEL

If the time evolution of the previous state $|\Psi_t\rangle$ is known, one can determine the expectation value of the atomic population inversion $\langle\Psi_t|S_3|\Psi_t\rangle$. However, in view of the analytical complexity of such state, a numerical approach would be required.

Here, as an application of our perturbative study of the TPM, we consider the simple case where the atomic population inversion involves the two states $|n\rangle|+1\rangle$ and $|m\rangle|-1\rangle$. The system constituted by either excited or unexcited atoms, each one corresponding to one such states, is then described by

$$|D(n,m)\rangle = \alpha|n\rangle|+1\rangle + \beta|m\rangle|-1\rangle, \tag{20}$$

with $1 = |\alpha|^2 + |\beta|^2$, whose time evolution is reported in Appendix B. The choice $m = n+2$ is made when considering the characteristic excitation/deexcitation processes described by the TPM interaction. Based on state (B1) one derives the time-dependent formula for the API $\langle S_3(t)\rangle_{nm} = \langle D_t(n,m)|S_3|D_t(n,m)\rangle$ whose final form is

$$\begin{aligned}\langle S_3(t)\rangle_{nm} &= \tfrac{1}{2}|\alpha|^2(|A|^2 - |C_+|^2 - |C_-|^2)\\ &+ \tfrac{1}{2}|\beta|^2(-|A'|^2 + |C'_+|^2 + |C'_-|^2)\\ &+ \tfrac{1}{2}\bar\alpha\beta(\bar A C'_+\langle n|m+2\rangle + \bar A C'_-\langle n|m-2\rangle\\ &- A'\bar C_+\langle n+2|m\rangle - A'\bar C_-\langle n-2|m\rangle)\\ &+ \tfrac{1}{2}\alpha\bar\beta(-\bar A' C_+\langle m|n+2\rangle - \bar A' C_-\langle m|n-2\rangle\\ &+ A\bar C'_+\langle m+2|n\rangle + A\bar C'_-\langle m-2|n\rangle).\end{aligned} \tag{21}$$

By exploiting the coefficients reported in Appendix B, the latter reduces, for $m = n+2$, to the final form (we set, for brevity, $\langle S_3(t)\rangle_{n\,n+2} = \langle S_3(t)\rangle$)

$$\begin{aligned}\langle S_3(t)\rangle &= \frac{1}{2}(|\alpha|^2 - |\beta|^2) + \varepsilon\frac{q(-1)}{2\sqrt{2}}\sqrt{\binom{n+2}{2}}[\bar\alpha\,\beta\,(e^{-it\omega_0\varepsilon^2\eta_n} + e^{-it\omega_0\varepsilon^2\eta_{n+2}})(e^{-i2(\omega-\omega_0/2)t} - 1) + \text{c.c.}] - 2\varepsilon^2q^2(1)\\ &\times\left[|\alpha|^2\binom{n}{2} - |\beta|^2\binom{n+4}{2}\right]\sin^2[(\omega+\omega_0/2)t] - 2\varepsilon^2q^2(-1)\binom{n+2}{2}(|\alpha|^2 - |\beta|^2)\,\sin^2[(\omega-\omega_0/2)t],\end{aligned} \tag{22}$$

where $\eta_n = \omega_0^2(n^2+n+1)/(4\omega^2 - \omega_0^2)$. In view of prospective experimental studies, we emphasize that the significant time scale in Eq. (22) is given by $t \sim T_\pm \ll T_\varepsilon$. In this case, formula (22) considerably simplifies, since the exponential terms depending on $\Delta E_2(m \pm q, \pm r)$ essentially reduce to 1. One finds

$$\begin{aligned}\langle S_3(t)\rangle &= \frac{|\alpha|^2 - |\beta|^2}{2} - \frac{\varepsilon q(-1)}{\sqrt{2}}\sqrt{\binom{n+2}{2}}\{\alpha^*\beta + \alpha\beta^* - 2|\alpha\beta|\cos[(\omega_0 - 2\omega)t - \Delta\theta]\} - 2\varepsilon^2q^2(1)\sin^2\left(\frac{2\omega+\omega_0}{2}t\right)\\ &\times\left[|\alpha|^2\binom{n}{2} - |\beta|^2\binom{n+4}{2}\right] - 2\varepsilon^2q^2(-1)\sin^2\left(\frac{2\omega-\omega_0}{2}t\right)\binom{n+2}{2}(|\alpha|^2 - |\beta|^2),\end{aligned} \tag{23}$$

where $\xi = |\xi|e^{i\theta_\xi}, \xi = \alpha,\beta$, and $\Delta\theta = \theta_\alpha - \theta_\beta$. As a reference case, we illustrate Eq. (23) in Fig. 1 for the simplest possible choice of the population parameters $|\alpha|^2 = |\beta|^2$ (equal populations) and $\Delta\theta = 0$ (coherent phases). Next, we show in Fig. 2 the results corresponding to a parameter choice where, due the assumption of different populations, both the second-order contributions are present. In all figures, on the time axis the rescaled time $\omega_0 t$ is represented.

Discussion. Various interesting cases relevant to Eq. (23) can be found by varying the field frequency ω with respect to the atomic transition energy ω_0.

In the near-resonance regime ω is close to $\omega_0/2$ so that, remembering definition (15), the quantity $|q(-1)|$ can be made significantly larger than $q(+1)$. The choice of $2\omega - \omega_0$ is made, of course, to avoid affecting the perturbative character of $\varepsilon^2q(-1)$ by the potentially diverging behavior of $q(-1)$

when $\omega \to \omega_0/2$. Then, by neglecting the $q(+1)$-dependent term (this, in addition, is fast oscillating with respect to the $q(-1)$-dependent term) the API reads

$$\langle S_3(t)\rangle \simeq \frac{|\alpha|^2-|\beta|^2}{2} - \frac{\varepsilon q(-1)}{\sqrt{2}}\sqrt{\binom{n+2}{2}} \times 4|\alpha\beta| \times\left\{-\sin^2\left(\frac{\Delta\theta}{2}\right)+\sin^2\left[\frac{(\omega_0-2\omega)t-\Delta\theta}{2}\right]\right\} -2\varepsilon^2 q^2(-1)\sin^2\left(\frac{2\omega-\omega_0}{2}t\right)\binom{n+2}{2} \times(|\alpha|^2-|\beta|^2),$$

where the cosine term of (23) has been rewritten according to the formula $\cos\eta = 1-2\sin^2(\eta/2)$. The new expression of $\langle S_3(t)\rangle$ still exhibits an explicit dependence on the coherence property of the atomic population through the parameter $\Delta\theta$ and features an evident phenomenon of collapses and revivals.

The time scale of the latter is controlled by the period $T = 4\pi/|2\omega-\omega_0|$ to both the first and second perturbative order. However, the pulses of the first-order term are characterized by the delay time $T\Delta\theta/4\pi$ with respect to that emerging from the second-order term. If, in addition, coherent atomic populations are considered, namely, if $\theta_\alpha = \theta_\beta$, the API remarkably simplifies, giving

$$\langle S_3(t)\rangle \simeq \frac{|\alpha|^2-|\beta|^2}{2} - 2\varepsilon\Lambda_n \sin^2\left[\frac{(\omega_0-2\omega)t}{2}\right],$$

with

$$\Lambda_n = q(-1)\frac{(n+2)!}{n!}\left[\frac{|\alpha\beta|\sqrt{n!}}{\sqrt{(n+2)!}} + \frac{\varepsilon}{2}q(-1)(|\alpha|^2-|\beta|^2)\right].$$

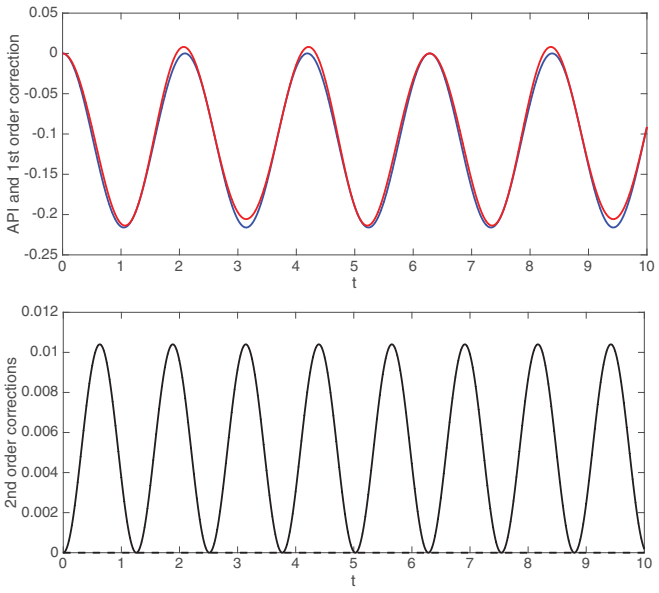

FIG. 1. API for the TPM. Upper panel: API [red (light gray) line] and first-order contribution [blue (dark gray) line] described by Eq. (23) for $|\alpha|^2 = |\beta|^2 = 0.5$, $\omega = 2$, $g = 0.1$, $\Delta\theta = 0$ and $n = 5$ (energies in units of ω_0). Lower panel: since $|\alpha|^2 = |\beta|^2$ only the first second-order term of Eq. (23) contributes.

This sensitivity to the changes of parameter $\Delta\theta$ should be interesting in view of experimental observations.

A second interesting case is found when restoring the off-resonance condition and setting $|\alpha|^2 = |\beta|^2 = 1/2$ in Eq. (23). This equality amounts to assuming identical atomic populations in (20). In this case we find

$$\langle S_3(t)\rangle = \varepsilon\Xi_n\left\{\sin^2(\Delta\theta/2) - \sin^2\left[\frac{(\omega_0-2\omega)t-\Delta\theta}{2}\right]\right\} + 2\varepsilon^2 q^2(1)(2n+3)\sin^2\left(\frac{2\omega+\omega_0}{2}t\right), \quad (24)$$

with $\Xi_n = \sqrt{2}q(-1)\binom{n+2}{2}^{1/2}$, highlighting an oscillation modality where the perturbative terms dictate the time behavior of the API. Note that Eq. (24) holds as well in the extreme regimes $\omega \gg \omega_0$ and $\omega \ll \omega_0$. It is worth observing that in the latter case the API signal exhibits amplitude and period essentially independent from frequency ω. On the other hand, for $\omega \gg \omega_0$, the amplitude of the API is proportional to the ratio $\omega_0/2\omega$ (the second-order term becomes rapidly negligible) while the period of the API pulses is essentially controlled by ω.

Finally, restoring the near-resonance case, we report the numerical results obtained from the general equation (23) in Fig. 3, where the effect of considering equal or different populations for noncoherent phases, $\Delta\theta = \pi/2$, is highlighted. The suppression of zero-order and of one of the two second-order

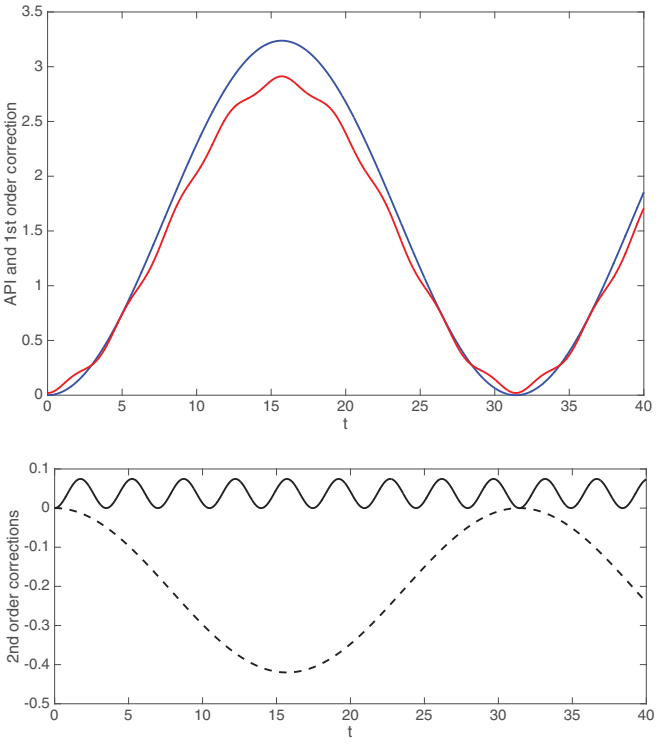

FIG. 2. API for the TPM. Upper panel: API [red (light gray) line] and first-order contribution [blue (dark gray) line] described by Eq. (23) for $|\alpha|^2 = 0.52$, $|\beta|^2 = 0.48$, $\omega = 0.4$, $g = 0.1$, $\Delta\theta = 0$ and $n = 5$ (energies in units of ω_0). Lower panel: second-order contributions, first (second) term in Eq. (23) corresponds to the solid (dashed) line.

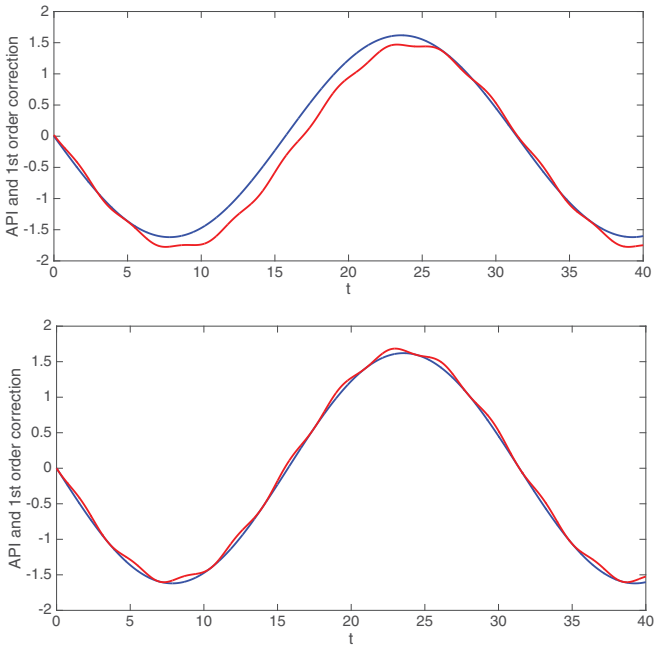

FIG. 3. API [red (light gray) line] and the first-order contribution [blue (dark gray) line] of the TPM for $\omega = 0.4$, $g = 0.1$ and $\Delta\theta = \pi/2$ (energies in units of ω_0). Upper panel: $|\alpha|^2 = 0.52$, $|\beta|^2 = 0.48$. Lower panel: $|\alpha|^2 = |\beta|^2 = 0.5$.

contributions, caused by $|\alpha|^2 = |\beta|^2$, is clearly visible in the lower panel of Fig. 3.

VI. PERTURBATIVE RESULTS FOR THE INTENSITY-DEPENDENT MODEL

Since the unperturbed Hamiltonian $H_{\rm unp}$ is the same for both the TPM and the IDM, the zeroth-order eigenvalues and eigenvectors are still given by Eqs. (12). Similar to the TPM, for the IDM the first-order contribution to the energy is $E_1(n,s) = 0$, while for the eigenstate one finds

$$|E_1(n,s)\rangle = \omega_0\left[\frac{f^2(n)|n-1\rangle}{\omega+\omega_0 s} - \frac{f^2(n+1)|n+1\rangle}{\omega-\omega_0 s}\right]|-s\rangle,$$

with $f(n) = \sqrt{n(n+2\kappa-1)}$. The second-order contributions to eigenvalues and eigenvectors read

$$E_2(n,s) = \omega_0^2\left[\frac{n(n+2\kappa-1)}{\omega+\omega_0 s} + \frac{(n+1)(n+2\kappa)}{-\omega+\omega_0 s}\right] \quad (25)$$

and

$$|E_2(n,s)\rangle = \frac{\omega_0}{2\omega}(q(s)F_n|n-2\rangle + q(-s)F_{n+2}|n+2\rangle)|s\rangle,$$

respectively, with $F_n = f(n-1)f(n)$. Clearly, the presence of level doublets in the energy spectrum also emerges in the IDM in the two regimes $\omega_0 = p\omega$ (with integer $p > 1$) and $\omega_0 \ll \omega$. The energy gaps relevant to such doublets are easily calculated along the same lines of the TPM (see Sec. III A).

The distinctive feature of the IDM is the presence of parameter κ, which presently has no direct physical interpretation. However, in the limit $\kappa \to \infty$, this parameter allows one to reduce [see the ladder-operator definitions (3)] the IDM to the single-photon quantum Rabi model (SPM). (The factor $\sqrt{\kappa}$ emerging from the limit can be absorbed in the interaction g.) If one considers the eigenvalue $E(n,s) = E_0(n,s) + \varepsilon^2 E_2(n,s)$ with $\varepsilon = g/\omega_0$ and $\kappa \to \infty$, the second-order contributions of the SPM,

$$\varepsilon^2 E_2(n,s) = 2(g\sqrt{\kappa})^2\left[\frac{n}{\omega+\omega_0 s} + \frac{(n+1)}{-\omega+\omega_0 s}\right], \quad (26)$$

show a dramatic change, from quadratic to linear, in the dependence from the photon number n with respect to the case with finite κ. Conversely, for small κ, formula (25) essentially coincides with formula (14), displaying a dependence on n^2 for $n \gg 1$. Then, in this case, almost no difference arises between the spectrum of the IDM and that of the TPM, even if the first model involves single-photon instead of two-photon processes.

The intermediate regime where κ is large enough (but finite) becomes interesting for $0 \leqslant n < \kappa$. In this interval, Eq. (25) shows a well-visible deviation from the quadratic dependence on n, which assumes the n-linear form (26). The quadratic dependence on n is recovered for $n > \kappa$. This effect should be accessible to the experimental observation in the recently realized waveguide superlattices [23–25], reproducing the matter-radiation coupling of the IDM for $\kappa = 1/2$.

A. Atomic population inversion within the intensity-dependent model

In view of the different coupling scheme displayed by the IDM, where a single photon (rather than two) is involved in the energy exchanges, we consider the atomic population inversion for a system whose atoms initially are in one of the two states $|n\rangle|+1\rangle$ and $|n+1\rangle|-1\rangle$. The time evolution of the elementary states $|m,r\rangle$ is required to derive the expectation value describing the API. All relevant calculations are reported in Appendix C.

Despite the difference in the initial state, the structure of the API for the present model closely mimics the one obtained in the two-photon case. By exploiting the time-evolved state (C1) one readily obtains $|D_t(m,n)\rangle = \alpha|\phi_t(n,+1)\rangle + \beta|\phi_t(m,-1)\rangle$, with $m = n+1$, connected to the initial state $\alpha|n\rangle|+1\rangle + \beta|n+1\rangle|-1\rangle$. As in the TPM case, one then determines the expectation value $\langle S_3(t)\rangle = \langle D_t(m,n)|S_3|D_t(m,n)\rangle$ whose general expression (D2) is derived in Appendix D. By observing that, as suggested by Eqs. (C1) and (D2), the time scales of the ID model are

$$T_\pm = \frac{2\pi}{|\omega_0 \pm \omega|} \ll T_\epsilon \sim \frac{2\pi}{\varepsilon^2 \Delta E_2(m \pm q, \pm r)}, \quad (27)$$

for observation times $t \sim T_\pm$ Eq. (D2) reduces to the simple form

$$\begin{aligned}\langle S_3(t)\rangle = {} & \frac{|\alpha|^2 - |\beta|^2}{2} - \varepsilon q(-1) f(n+1)\{\alpha^*\beta + \alpha\beta^* \\ & -2|\alpha\beta|\cos[(\omega_0-\omega)t - \Delta\theta)]\} - 4\varepsilon^2 q^2(1) \\ & \times \sin^2\left(\frac{\omega+\omega_0}{2}t\right)[|\alpha|^2 f^2(n) - |\beta|^2 f^2(n+2)] \\ & -4\varepsilon^2 q^2(-1)\sin^2\left(\frac{\omega-\omega_0}{2}t\right) f^2(n+1)(|\alpha|^2 - |\beta|^2),\end{aligned} \quad (28)$$

with $q(r) = \omega_0/(\omega + r\omega_0)$, since the ε^2-dependent exponentials in Eq. (D2) become essentially equal to 1.

Discussion. We note that the considerations and results pertaining to the TPM discussion can be extended to the IDM with slight modifications. For example, the quantity $|q(-1)|$ can be made significantly larger than $q(+1)$ in the near-resonance regime ($\omega \simeq \omega_0$). In this case, Eq. (28) reads

$$\langle S_3(t)\rangle = \frac{|\alpha|^2 - |\beta|^2}{2} - \varepsilon q(-1) f(n+1) 4|\alpha\beta| \times \left\{ -\sin^2\left(\frac{\Delta\theta}{2}\right) + \sin^2\left[\frac{(\omega_0 - \omega)t - \Delta\theta}{2}\right]\right\} - 4\varepsilon^2 q^2(-1)\sin^2\left(\frac{\omega - \omega_0}{2}t\right) \times f^2(n+1)(|\alpha|^2 - |\beta|^2).$$

As for the near-resonance regime of the TPM, also this expression exhibits an explicit dependence from the initial phases θ_α and θ_β of the two amplitudes α, β of $|D_t(n+1,n)\rangle$ at $t = 0$. The time scale characterizing the pulses of $\langle S_3\rangle$ is $T' = 4\pi/|\omega - \omega_0|$ (the delay time between the first- and second-order terms is still given by $T'\Delta\theta/4\pi$), while the condition $\Delta\theta = 0$ for coherent atomic populations implies

$$\langle S_3(t)\rangle = \frac{|\alpha|^2 - |\beta|^2}{2} - 4\varepsilon\Lambda_n(\kappa)\sin^2\left[\frac{(\omega_0 - \omega)t}{2}\right],$$

with

$$\Lambda_n(\kappa) = q(-1) f^2(n+1) \times \left[\frac{|\alpha\beta|}{f(n+1)} + \varepsilon q(-1)(|\alpha|^2 - |\beta|^2)\right].$$

In the off-resonance condition and for equal population, $|\alpha|^2 = |\beta|^2 = 1/2$, the analogue of Eq. (24) is

$$\langle S_3(t)\rangle = \varepsilon\Xi'_n\left\{\sin^2(\Delta\theta/2) - \sin^2\left[\frac{(\omega_0 - \omega)t - \Delta\theta}{2}\right]\right\} + 4\varepsilon^2 q^2(1)(2n + 2\kappa + 1)\ \sin^2\left(\frac{\omega + \omega_0}{2}t\right), \tag{29}$$

where $\Xi'_n = q(-1)f(n+1)$, and $f(n) = \sqrt{n(n+2\kappa-1)}$. Equation (29) discloses an oscillation modality where the perturbative terms dominate the time behavior of the API. The same comments made for the API of the TPM when either $\omega \ll \omega_0/2$ or $\omega \gg \omega_0/2$ can be extended to the present case.

The dependence on an (in principle) arbitrary parameter κ indeed represents a new aspect characterizing the IDM. Small values of κ have an essentially negligible effect on the API of the IDM, which displays the same linear dependence of the TPM on the photon number n. Conversely, for large values of κ, the diversity of the TPM and of the IDM becomes fully evident. The comparison of Eqs. (24) and (29) shows that, for $n/(2\kappa) < 1$, the API of the TPM is controlled by a factor $\sqrt{(n+1)(n+2)} \approx n$, while for the IDM this factor becomes $\sqrt{\kappa(n+1)}$. This behavior is illustrated in Fig. 4 for small ($n = 1,5$) and large ($n = 120$) photon numbers with $\kappa = 20$.

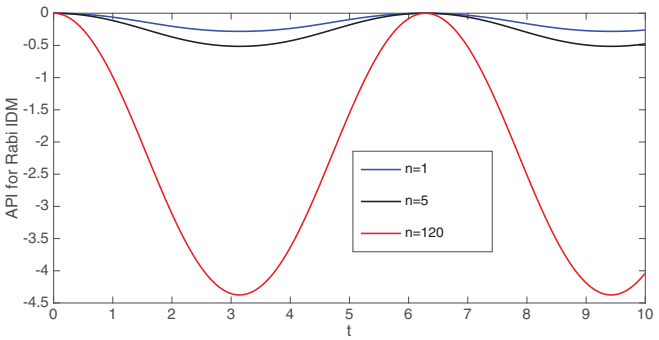

FIG. 4. API of the IDM for different photon numbers, $n = 1$ [blue (dark gray) line], $n = 5$ (black line), and $n = 120$ [red (light gray) line]. $\kappa = 20$, $|\alpha|^2 = |\beta|^2 = 0.5$, $\omega = 2$, $g = 0.0016$ and $\Delta\theta = 0$ (energies in units of ω_0).

VII. CONCLUSIONS

We have applied the perturbation method to both the two-photon and intensity-dependent Rabi models, determining the eigenvalues and the corresponding eigenstates to the second order in the parameter g/ω_0. Based on this analysis, we have calculated the time evolution of the product of a photonic and an atomic state $|m\rangle|r\rangle$. We have utilized this result to derive the expectation value of the atomic population inversions, the latter including all the physical parameters embedded in the Rabi Hamiltonians, as well as the phases and amplitudes of the initial states $|D(m,n)\rangle$ representing the superposition of two atomic states with appropriate photon numbers.

Our analysis highlights a strong similarity between TPM and IDM (with finite κ) as far as the eigenvalues, the eigenstates, the time-evolved state $|D_t(m,n)\rangle$, and the API $\langle S_3(t)\rangle$ are concerned. For large values of κ the diversity of the two models appears both in the second-order energy contributions and in the oscillating-term amplitude of $\langle S_3(t)\rangle$. Note that our results depend on significant physical parameters such as (i) the frequency ratios $\omega_0/2\omega$ or ω_0/ω in the TPM or IDM case, respectively, controlling the near- and far-resonance regimes, (ii) the phase difference $\Delta\theta$ in the atomic components of $|D(m,n)\rangle$, and (iii) the fractions $|\alpha|^2$ and $|\beta|^2$ of the atomic populations. Our perturbative analysis then offers a scheme in which the explicit dependence on the model parameters favors the experimental study of their interplay and of the influence on the time evolution of the system (for example, through the API).

Finally, the results about the IDM provide new information concerning the dynamics of the waveguide superlattices mentioned in the Introduction, the link between the latter and the IDM being obtained for $\kappa = 1/2$. In this case, the Schrödinger problem of the IDM coincides with the dynamical equations of waveguide superlattices.

ACKNOWLEDGMENT

This work has been supported by MIUR (Grant No. PRIN 2010LLKJBX).

APPENDIX A: TIME EVOLUTION OF UNPERTURBED ENERGY EIGENSTATE FOR THE TPM

To determine the formula describing the time evolution of a generic state $|m\rangle|r\rangle$ including second-order corrections, we exploit the completeness of the energy-state basis $\{|E(m,r)\rangle\}$. This allows one to represent the identity operator as

$$\mathbb{I} = \sum_n \sum_s |E(n,s)\rangle\langle E(n,s)|,$$

and thus to describe the time propagation of $|m\rangle|r\rangle$ by means of

$$e^{-iHt}|m\rangle|r\rangle = \sum_n \sum_s e^{-iE(n,s)t}\langle E(n,s)|m\rangle|r\rangle\ |E(n,s)\rangle.$$

Within the second-order approximation the eigenstates are given by

$$|E(n,s)\rangle = R(n,s)(|E_0(n,s)\rangle + \varepsilon|E_1(n,s)\rangle + \varepsilon^2|E_2(n,s)\rangle),$$

where the normalization factor

$$R(n,s) = 1/(1+\varepsilon^2\langle E_1(n,s)|E_1(n,s)\rangle)^{1/2}$$

has been included, and the eigenvalues are

$$E(n,s) = E_0(n,s) + \varepsilon^2 E_2(n,s).$$

Then, by defining $|\psi_t(m,r)\rangle = e^{-iHt}|m\rangle|r\rangle$, one finds

$$\begin{aligned}
|\psi_t(m,r)\rangle = e^{-iE(m,r)t}&\left\{|m\rangle|r\rangle + \varepsilon|E_1(m,r)\rangle + \varepsilon^2|E_2(m,r)\rangle - \frac{\varepsilon^2}{2}\left[q^2(r)\binom{m}{2} + q^2(-r)\binom{m+2}{2}\right]|m\rangle|r\rangle\right\}\\
&+\varepsilon\frac{1}{\sqrt{2}}\left[e^{-iE(m+2,-r)t}q(-r)\binom{m+2}{2}^{\frac{1}{2}}|m+2\rangle|-r\rangle - e^{-iE(m-2,-r)t}q(r)\binom{m}{2}^{\frac{1}{2}}|m-2\rangle|-r\rangle\right]\\
&+\varepsilon^2\frac{1}{\sqrt{2}}\left[e^{-iE(m+2,-r)t}q(-r)\binom{m+2}{2}^{\frac{1}{2}}|E_1(m+2,-r)\rangle - e^{-iE(m-2,-r)t}q(r)\binom{m}{2}^{\frac{1}{2}}|E_1(m-2,-r)\rangle\right]\\
&+\varepsilon^2\frac{\sqrt{6}}{8}\frac{\omega_0}{\omega}\left[e^{-iE(m+4,r)t}q(r)\binom{m+4}{4}^{\frac{1}{2}}|m+4\rangle|r\rangle + e^{-iE(m-4,r)t}q(-r)\binom{m}{4}^{\frac{1}{2}}|m-4\rangle|r\rangle\right].
\end{aligned} \tag{A1}$$

The final form of this state, where the contributions relevant to the first and the second perturbative order are grouped in separated terms, is given in Eq. (18).

APPENDIX B: TIME EVOLUTION OF STATES $|D(m,n)\rangle$

The evolved state (A1) is the basic element for determining the time evolution of the initial mixed state (20). This, in turn, allows one to calculate the time behavior of the API for the TPM. The time evolution of state (20) is described by

$$\begin{aligned}
|D_t(m,n)\rangle = e^{-iHt}(\alpha|n\rangle|1\rangle + \beta|m\rangle|-1\rangle) &= \alpha(A(n,t)|n\rangle|+1\rangle + B_+(n,t)|n+4\rangle|+1\rangle\\
&+ B_-(n,t)|n-4\rangle|+1\rangle + C_+(n,t)|n+2\rangle|-1\rangle + C_-(n,t)|n-2\rangle|-1\rangle) + \beta(A'(m,t)|m\rangle|-1\rangle\\
&+ B'_+(m,t)|m+4\rangle|-1\rangle + B'_-(m,t)|m-4\rangle|-1\rangle + C'_+(m,t)|m+2\rangle|+1\rangle + C'_-(m,t)|m-2\rangle|+1\rangle),
\end{aligned} \tag{B1}$$

where

$$A(n,t) = e^{-iE(n,1)t}\left\{1-\varepsilon^2\left[\frac{1}{2}\left(q^2(1)\binom{n}{2} + q^2(-1)\binom{n+2}{2}\right)\right] + \varepsilon^2\frac{1}{2}\left[q^2(-1)\binom{n+2}{2}e^{i(\omega_0-2\omega)t} + q^2(1)\binom{n}{2}e^{i(\omega_0+2\omega)t}\right]\right\},$$

$$\begin{aligned}
A'(m,t) = e^{-iE(m,-1)t}&\left\{1-\varepsilon^2\left[\frac{1}{2}\left(q^2(-1)\binom{m}{2} + q^2(1)\binom{m+2}{2}\right)\right] + \varepsilon^2\frac{1}{2}\left[q^2(1)\binom{m+2}{2}e^{-i(\omega_0+2\omega)t}\right.\right.\\
&\left.\left.+ q^2(-1)\binom{m}{2}e^{i(-\omega_0+2\omega)t}\right]\right\},
\end{aligned}$$

$$B_\pm(n,t) = \varepsilon^2\frac{\sqrt{6}}{8}\frac{\omega_0}{\omega}e^{-iE(n\pm4,1)t}\sqrt{\binom{n+2\pm2}{4}}[q(\mp1)e^{\pm i4\omega t} + q(\pm1)],$$

$$B'_\pm(m,t) = \varepsilon^2\frac{\sqrt{6}}{8}\frac{\omega_0}{\omega}e^{-iE(m\pm4,-1)t}\sqrt{\binom{m+2\pm2}{4}}[q(\pm1)e^{\pm i4\omega t} + q(\mp1)],$$

$$C_{\pm}(n,t) = \mp\frac{\varepsilon}{\sqrt{2}} e^{-iE(n\pm 2,1)t} q(\mp 1)\sqrt{\binom{n+1\pm 1}{2}}(e^{\pm i2\omega t} - e^{i\omega_0 t}),$$

$$C'_{\pm}(m,t) = \mp\frac{\varepsilon}{\sqrt{2}} e^{-iE(m\pm 2,-1)t} q(\pm 1)\sqrt{\binom{m+1\pm 1}{2}}(e^{\pm i2\omega t} - e^{-i\omega_0 t}).$$

APPENDIX C: TIME EVOLUTION OF STATES $|m,r\rangle$ AND $|D(m,n)\rangle$ FOR THE IDM

The time evolution of a state $|m,r\rangle$ is driven by the IDM Hamiltonian. Its time evolution can be calculated along the same lines followed to obtain state (18) for the TPM. The details of this calculation are reported in Appendix A, leading to formula (A1). With a long but straightforward calculation the evolved state $|\phi_t(m,r)\rangle = e^{-iHt}|m,r\rangle$ is found to be

$$\begin{aligned}|\phi_t(m,r)\rangle &= e^{-iE(m,r)t}[1+\varepsilon^2\tilde{V}_t(r,m,\varepsilon)+\varepsilon^2\tilde{V}'_t(r,m,\varepsilon)]|m\rangle|r\rangle \\ &+\varepsilon^2 e^{-iE(m,r)t}[e^{2i\omega t}\tilde{U}_t(r,m,\varepsilon)|m-2\rangle|r\rangle + e^{-2i\omega t}\tilde{U}'_t(r,m,\varepsilon)|m+2\rangle|r\rangle] \\ &+\varepsilon e^{-iE(m,r)t}(1-e^{i(\omega+r\omega_0-\varepsilon^2\Delta E_2(m-1,-r))t})q(r)f(m)|m-1\rangle|-r\rangle \\ &-\varepsilon e^{-iE(m,r)t}(1-e^{i(r\omega_0-\omega+\varepsilon^2\Delta E_2(m+1,-r))t})q(-r)f(m+1)|m+1\rangle|-r\rangle, \end{aligned} \tag{C1}$$

where

$$\begin{aligned}\tilde{V}_t(r,m,\varepsilon) &= q^2(r)f^2(m)(e^{i(\omega+r\omega_0-\varepsilon^2\Delta E_2(m-1,-r))t}-1), \\ \tilde{V}'_t(r,m,\varepsilon) &= q^2(-r)f^2(m+1)(e^{-i(\omega-r\omega_0-\varepsilon^2\Delta E_2(m+1,-r))t}-1), \\ \tilde{U}_t(r,m,\varepsilon) &= \chi_{m-1}\left[\frac{\omega_0}{2\omega}(q(r)e^{-2i\omega t}+e^{-i\varepsilon^2\Delta E_2(m-2,r)t}q(-r)) - q(-r)q(r)e^{-i(\omega-r\omega_0+\varepsilon^2\Delta E_2(m-1,-r))t}\right], \\ \tilde{U}'_t(r,m,\varepsilon) &= \chi_{m+1}\left[\frac{\omega_0}{2\omega}(q(-r)e^{2i\omega t}+e^{-i\varepsilon^2\Delta E_2(m+2,r)t}q(r)) - q(r)q(-r)e^{i(\omega+r\omega_0-\varepsilon^2\Delta E_2(m+1,-r))t}\right],\end{aligned}$$

with $\chi_m = f(m+1)f(m)$, and

$$\Delta E_2(n\pm q,-r) = E_2(n\pm q,-r) - E_2(n,r)$$

[see formula (25)]. Once more, we observe that, within the second-order approximation, the energy eigenvalues are given by $E(n,s) = E_0(n,s) + \varepsilon^2 E_2(n,s)$. Interestingly, we note how, in spite of the different algebraic structures characterizing the IDM and the TPM coupling, the time-evolved state (C1) exhibits the same structure of the two-photon counterpart (18).

APPENDIX D: ATOMIC POPULATION INVERSION FOR THE IDM

The formula describing the time evolution of the API for the IDM is readily derived by using the time-evolved state $|D_t(m,n)\rangle = e^{-itH}|D(m,n)\rangle = e^{-itH}(\alpha|n\rangle|+1\rangle + \beta|m\rangle|-1\rangle)$ and states $|\phi_t(n,r)\rangle = e^{-itH}|n\rangle|r\rangle$ given by formula (C1). We then obtain

$$\langle D_t(m,n)|S_3|D_t(m,n)\rangle = \frac{1}{2}|\alpha|^2(|A|^2-|C_+|^2-|C_-|^2) + \frac{|\beta|^2}{2}(|C'_+|^2+|C'_-|^2-|A'|^2) + \left(\frac{\bar{\alpha}\beta}{2}\,\Omega_{m,n} + \text{c.c.}\right), \tag{D1}$$

where

$$\Omega_{m,n} = \bar{A}C'_+\langle n|m+1\rangle + \bar{A}C'_-\langle n|m-1\rangle - A'\bar{C}_+\langle n+1|m\rangle - A'\bar{C}_-\langle n-1|m\rangle$$

and

$$\begin{aligned}A(n,t) &= e^{-iE(n,1)t}\{1-\varepsilon^2[(q^2(1)f^2(n)+q^2(-1)f^2(n+1)) - q^2(-1)f^2(n+1)e^{i(\omega_0-\omega)t} - q^2(1)f^2(n)e^{i(\omega_0+\omega)t}]\}, \\ A'(m,t) &= e^{-iE(m,-1)t}\{1-\varepsilon^2[(q^2(-1)f^2(m)+q^2(1)f^2(m+1)) - q^2(1)f^2(m+1)e^{-i(\omega_0+\omega)t} - q^2(-1)f^2(m)e^{i(\omega-\omega_0)t}]\}, \\ B_{\pm}(n,t) &= \varepsilon^2 e^{-itE(n,1)}f(n\pm 1)f(n+1\pm 1)\left\{\frac{\omega_0}{2\omega}[q(-1)+q(+1)e^{\mp 2i\omega t}] - q(1)q(-1)e^{it(\omega_0\mp\omega)}\right\}, \\ B'_{\pm}(m,t) &= \varepsilon^2 e^{-itE(m,-1)}f(m\pm 1)f(m+1\pm 1)\left\{\frac{\omega_0}{2\omega}[q(\pm 1)+q(\mp 1)e^{\mp 2i\omega t}] - q(1)q(-1)e^{-it(\omega_0\pm\omega)}\right\}, \\ C_{\pm}(n,t) &= \pm\varepsilon\, e^{-itE(n,+1)}\,(e^{it(\omega_0\mp\omega)}-1)q(\mp 1)f(n+1/2\pm 1/2), \\ C'_{\pm}(m,t) &= \pm\varepsilon\, e^{-itE(m,-1)}(e^{-it(\omega_0\pm\omega)}-1)q(\pm 1)f(m+1/2\pm 1/2).\end{aligned}$$

By means of straightforward calculations the API (D1) takes the final form

$$\langle S_3(t)\rangle \equiv \langle D_t(m,n)|S_3|D_t(m,n)\rangle = \frac{|\alpha|^2-|\beta|^2}{2} - 4\varepsilon^2\Bigg[(|\alpha|^2-|\beta|^2)q^2(-1)f^2(n+1)\sin^2\left(\frac{\omega-\omega_0}{2}t\right) + q^2(1)\sin^2\left(\frac{\omega+\omega_0}{2}t\right)(|\alpha|^2 f^2(n)-|\beta|^2 f^2(n+2))\Bigg] + \left\{\frac{\varepsilon}{2}\alpha^*\beta e^{-i(\omega-\omega_0)t}e^{-i\varepsilon^2\Delta E_2(n+1,-1)t}q(-1)f(n+1)2[1-e^{i(\omega-\omega_0)t}]+\text{c.c.}\right\}, \quad \text{(D2)}$$

with $\Delta E_2(n\pm q,-r) = E_2(n\pm q,-r) - E_2(n,r)$ [see formula (25)], $r=1$, and $q=1$. It is worth noting how these time-dependent quantities exhibit the same form characterizing the analogous quantities of the TPM case defined below Eq. (B1).

[1] I. I. Rabi, Phys. Rev. **49**, 324 (1936); **51**, 652 (1937).
[2] L. Allen and J. H. Eberly, *Optical Resonance and Two-Level Atoms* (Dover Publications, New York, 1987).
[3] L. Mandel and E. Wolf, *Optical Coherence and Quantum Optics* (Cambridge University Press, Cambridge, UK, 1995).
[4] M. A. Nielsen and I. L. Chuang, *Quantum Computation and Quantum Information* (Cambridge University Press, Cambridge, UK, 2000).
[5] M. Inguscio and L. Fallani, *Atom Physics: Precise Measurements and Ultracold Matter* (Oxford University Press, Oxford, UK, 2013).
[6] D. Braak, Phys. Rev. Lett. **107**, 100401 (2011).
[7] I. Travěnec, Phys. Rev. A **85**, 043805 (2012).
[8] Q.-H. Chen, C. Wang, S. He, T. Liu, and K.-L. Wang, Phys. Rev. A **86**, 023822 (2012).
[9] J. Peng, Z. Ren, G. Guo, G. Ju, and X. Guo, Eur. Phys. J. D **67**, 162 (2013).
[10] S. Felicetti, J. S. Pedernales, I. L. Egusquiza, G. Romero, L. Lamata, D. Braak, and E. Solano, Phys. Rev. A **92**, 033817 (2015).
[11] V. V. Albert, G. D. Scholes, and P. Brumer, Phys. Rev. A **84**, 042110 (2011).
[12] J. Schwinger, *On Angular Momentum* (1952), reprinted in *Quantum Theory of Angular Momentum*, edited by L. C. Biedenharn and H. Van Dam (Academic Press, New York, 1965).
[13] M. Brune, J. M. Raimond, P. Goy, L. Davidovich, and S. Haroche, Phys. Rev. Lett. **59**, 1899 (1987).
[14] Y. Ota, S. Iwamoto, N. Kumagai, and Y. Arakawa, Phys. Rev. Lett. **107**, 233602 (2011).
[15] C. Emary and R. F. Bishop, J. Phys. A: Math. Gen. **35**, 8231 (2002).
[16] T. Holstein and H. Primakoff, Phys. Rev. **58**, 1098 (1940).
[17] J. Katriel, A. I. Solomon, G. D'Ariano, and M. Rasetti, Phys. Rev. D **34**, 2332 (1986).
[18] E. T. Jaynes and F. W. Cummings, Proc. IEEE **51**, 89 (1963).
[19] B. Buck and C. V. Sukumar, Phys. Lett. A **81**, 132 (1981).
[20] V. Buzěk, Phys. Rev. A **39**, 3196 (1989).
[21] B. M. Rodríguez–Lara, F. Soto–Eguibar, A. Zárate Cárdenas, and H. Moya–Cessa, Opt. Express **21**, 12888 (2013).
[22] B. M. Rodríguez–Lara, J. Opt. Soc. Am. B **31**, 1719 (2014).
[23] F. Dreisow, A. Szameit, M. Heinrich, T. Pertsch, S. Nolte, A. Tünnermann, and S. Longhi, Phys. Rev. Lett. **102**, 076802 (2009).
[24] S. Longhi, Opt. Lett. **36**, 3407 (2011).
[25] A. Crespi, S. Longhi, and R. Osellame, Phys. Rev. Lett. **108**, 163601 (2012).
[26] C. F. Lo, Eur. Phys. J. D **68**, 173 (2014).
[27] C. Cohen-Tannoudji, B. Dui, and F. Laloë, *Quantum Mechanics* (Hermann, Paris, 1977), Vol. II.
[28] V. Penna and F. A. Raffa, J. Phys. B: At., Mol. Opt. Phys. **47**, 075501 (2014).
[29] Spin commutators: $[S_+,S_-]=2S_3$, $[S_3,S_\pm]=\pm S_\pm$; su(1, 1) commutators: $[K_-,K_+]=2K_3$, $[K_3,K_\pm]=\pm K_\pm$.
[30] W. M. Zhang, D. H. Feng, and R. Gilmore, Rev. Mod. Phys. **62**, 867 (1990).